This is a repository copy of *Dynamic Measurement of Low Contact Angles by Optical Microscopy*.

White Rose Research Online URL for this paper:
https://eprints.whiterose.ac.uk/138705/

Version: Accepted Version

Dynamic Measurement of Low Contact Angles by Optical Microscopy

James M. Campbell*, Hugo K. Christenson

School of Physics and Astronomy, University of Leeds, Woodhouse Lane, Leeds, LS2 9JT, United Kingdom. *Email: j.m.campbell@leeds.ac.uk

Keywords: droplets; optics; wetting; wettability; mica.

Precise measurement of contact angles is an important challenge in surface science, in the design and characterisation of materials and in many crystallisation experiments. Here we present a novel technique for measuring the contact angles of droplets between about 2° and 30°, with lowest experimental uncertainty at the lower end of this range, typically ±0.1°. The lensing effect of a droplet interface produces the appearance of bright circles in low-aperture light, whose diameter is related to the contact angle. The technique requires no specialised equipment beyond an ordinary optical microscope, and may be used to study the dynamic evolution of the contact angle in-situ during an experiment.

1 Introduction

Measurement of liquid-on-solid contact angles is an important problem across a diverse set of scientific disciplines, from aerospace engineering and crystallisation to botany and soil science, amongst many others. Knowledge of contact angles is vital for estimating adhesion in granular materials[1-2], and for calculating the strength of capillary forces which dominate water absorption and flow phenomena in porous media and granular packings[3-5]. The contact angle has profound effects on the dynamics of drop impact[6] and on the dewetting of surfaces[7]. It can be used to estimate surface energies[8-9], and as a convenient way to calculate the volume of small droplets.

The techniques for measuring contact angles are almost as diverse as the reasons for doing so[10-11]. Perhaps the most common – and arguably the simplest – is the sessile drop technique, in which a drop of liquid is observed side-on through a goniometer. The contact angle may then be measured directly, or inferred through analysis of the drop profile. This technique is popular for several reasons: it is simple to perform, it is reasonably accurate and it may observe dynamic changes in contact angle. In this paper we present a new technique which boasts this same set of strengths (plus a few of its own) and can be used to measure contact angles of liquid droplets using nothing but an ordinary optical microscope.

Our technique exploits the ability of a small droplet to act as a lens: either the surface as a reflective lens or the bulk as a refractive lens. We are not the first to use reflective or refractive lensing to measure contact angles. Allain et al. illuminated a droplet with a laser, which both

reflected and refracted bright circles onto screens[12]. The diameter of these circles depended on the contact angle at the droplet's edge. Zhang and Chao described a similar technique, and used interference fringes on the projection to infer the shape of the drop near the contact line[13-14], and Thomas et al. devised a more sophisticated version of the same experiment in the refractive mode, using an interferometer to infer the drop profile from the intensity distribution of the lensed light[15]. Others have used the lensing of light to measure contact angles in different ways[16-18]. These techniques, whilst functional and accurate, require specialised optical setups (typically involving lasers) which may not be feasible for many researchers, and may not be suitable for non-static droplets, or those contained within an experimental chamber.

The strength of our technique lies in its simplicity. When observed under a microscope in low-aperture reflected light, a droplet appears to have one or more concentric circles of bright light of well-defined diameter, as shown in Figure 1. The diameter of these is determined by the optical properties of both the droplet and the microscope. If the microscope's properties are known and the system understood, then the contact angle of the droplet may be inferred.

The technique has its limitations, as well as its strengths. It is suitable only for measuring relatively small contact angles (we do not recommend it outside the range 2–30°) and for relatively small droplets (diameter below about 4 mm), and it requires a flat substrate, of homogeneous contact angle on the length scale of the droplet. However otherwise it is a very versatile, precise and inexpensive technique. Here in this paper we first develop the theory underlying the technique before moving on to an experimental description. Results are presented of some experimental verification tests, before concluding with a discussion of its strengths and limitations in comparison to existing techniques.

2 Theory

A microscope objective accepts light only over a limited range of angles, up to a critical angle φ_c from the normal. This can be predicted from its numerical aperture NA:

$$NA = n_m \sin \varphi_c \tag{1}$$

where n_m is the refractive index of the medium. This has an important implication when observing a film of liquid under a microscope with reflected light, the surface of which is at an angle α to the horizontal: if α exceeds a critical value α_c, then the angle of reflected light φ_r will exceed φ_c and the film will appear dark. This may happen for two different modes of reflection: direct reflection from the surface of the liquid (the reflective mode), or refraction through the liquid surface followed by reflection from the substrate surface (the refractive mode). These are illustrated in Figure 2.

When looking at a droplet, α increases with increasing distance from the centre. Hence the droplet will appear bright in the centre and dark closer to the edge. If the illumination aperture is closed down to a pinhole (causing light to reach each point of the surface at a single well-defined incident angle φ_i), the boundary between bright and dark becomes sharp and distinct, having a

diameter d. The two modes of reflection produce two boundaries: one corresponding to the reflective mode, nearer to the centre, and one corresponding to the refractive mode, nearer to the contact line. Figure 1 shows photographs illustrating the effect. The lower the contact angle of the droplet, the closer the boundaries will approach the contact line. For sufficiently low contact angles, only the reflective mode boundary will be visible. For even lower contact angles no boundary will be visible and the droplet will appear entirely bright.

We shall use the superscripts l and r to refer to quantities specific to the reflective or the refractive mode, respectively. The drop diameter D and either d^l or d^r may be used to predict the contact angle θ. There are several ways of doing this, depending on the level of accuracy required. We shall start from the simplest, and work up to the most accurate.

We shall make two approximations common to all approaches: first, that the droplet is shaped as a spherical cap (true for sufficiently small droplets on a flat homogeneous surface, see Discussion), and second, that the incident light may be described as equivalent to illumination by a point source a distance $z_o n_m$ above the substrate (z_o being a measurable property of the microscope and objective).

2.1 Thin film approximation

Here, we shall make two more approximations: that the distance between the curved interface and the substrate is negligible, and that the angles involved are small enough to apply the paraxial approximation ($\sin x \approx \tan x \approx x$; $\cos x \approx 1 - \frac{1}{2}x^2$). This lets us derive very simple analytical expressions which are sufficiently accurate for calculating very small angles. Comparing their predictions to numerical solutions for water drops with D up to 2 mm, they are seen to be accurate to within 5% for θ below 15°, 2.5% for θ below 10° and 0.5% for θ below 5°, for a selection of objectives across both modes.

By finding the critical surface angle α_c at which $\varphi_r = \varphi_c$, we can find the contact angle by approximating the interface shape as a parabola. This means that $\alpha(r)$ is proportional to the distance r from the droplet centre, and as $\alpha(\frac{D}{2}) = \theta$ at the perimeter, we derive the expression

$$\frac{\alpha\left(\frac{d}{2}\right)}{\alpha\left(\frac{D}{2}\right)} = \frac{\alpha_c}{\theta} \approx \frac{d}{D}. \tag{2}$$

The angle of incident light φ_i (shown in Figure 2) may be expressed as

$$\varphi_i \approx \frac{r}{z_o n_m}. \tag{3}$$

For the reflective mode, the reflection condition at the surface is

$$\varphi_r = \varphi_i + 2\alpha \tag{4}$$

leading to the final expression

3

$$\theta \approx \frac{D}{2n_m}\left(\frac{NA}{d^l} - \frac{1}{2z_o}\right) \tag{5}$$

using the criteria that $\alpha = \alpha_c^l$ and $\varphi_r = \varphi_c$ at $r = \frac{1}{2}d^l$. For the refractive mode, we must consider the angle of light within the droplet, β (shown in Figure 2). Now we have to satisfy Snell's law as the light passes both into and out of the drop:

$$\frac{\alpha + \varphi_i}{\alpha - \beta} \approx \frac{\alpha + \varphi_r}{\alpha + \beta} \approx \frac{n}{n_m} \tag{6}$$

where n is the refractive index of the liquid (we assume throughout that $n > n_m$). Note that the refractive index of the substrate does not need to be known, as the change in refractive index at the liquid-substrate interface affects only the intensity - not the direction - of reflected light. Equation 6 leads to the relationship

$$\varphi_r \approx -\varphi_i + 2\left(\frac{n}{n_m} - 1\right)\alpha \tag{7}$$

in place of Equation 4, and hence to an expression of similar form to Equation 5:

$$\theta \approx \frac{D}{2n_m}\left(\frac{n}{n_m} - 1\right)^{-1}\left(\frac{NA}{d^r} + \frac{1}{2z_o}\right). \tag{8}$$

2.2 Lensing approximation

The thin film approximation is sufficiently accurate for most purposes for θ up to about 10°. But above this it begins to become increasingly inaccurate, primarily because it does not consider the thickness of the droplet. An alternative approach which is much more accurate at higher contact angles (at least for the reflective mode) is to approximate the droplet as a simple lens. In the reflective mode, the droplet surface is a divergent reflective lens which focuses the light source a distance s_o above the lens to a virtual image a distance s_i^l below the lens. In the refractive mode, the droplet acts as a double-convex converging refractive lens, focusing to a real image a distance s_i^r above it. Both modes are illustrated in Figure 3.

The observed bright region is the set of points on the focal plane (substrate surface) illuminated by the image of the light source at an angle to the vertical below the critical angle φ_c. Thus if z_i is the distance between the image and the focal plane, then

$$\tan \varphi_c = \frac{d}{2z_i}. \tag{9}$$

In the reflective mode, the lens is modelled as a thin lens located at the apex of the drop, a distance h above the surface, where

4

$$h = R(1 - \cos\theta), \tag{10}$$

R being the radius of curvature given by

$$R = \frac{D}{2\sin\theta}. \tag{11}$$

The object and image distances are therefore $s_o = z_o - h$ and $s_i^l = z_i^l + h$. These are related by the thin lens equation

$$\frac{1}{s_0} - \frac{1}{s_i^l} = \frac{1}{f^l} \tag{12}$$

where f^l is the (negative) focal length of the reflective surface, given by

$$f^l = -\frac{R}{2}. \tag{13}$$

Combining these equations:

$$\frac{1}{z_o - h} - \frac{1}{\dfrac{d^l}{2\tan\varphi_c} + h} = -\frac{2}{R} \tag{14}$$

which, upon rearranging and substituting Equations 10 and 11, gives

$$d^l = 2\tan\phi_c \left(\left[\frac{4\sin\theta}{D} + \frac{1}{z_o - Df(\theta)} \right]^{-1} - Df(\theta) \right) \tag{15}$$

where

$$f(\theta) = \frac{1 - \cos\theta}{2\sin\theta}. \tag{16}$$

Thus d^l can be calculated from D and θ for a known ϕ_c and z_o. Unlike for the thin film approximation, this does not work in reverse: θ cannot be expressed in terms of d^l and D. Figure 4 shows the predictions of this approximation compared to numerical solutions, for a water droplet with $D = 2$ mm. Agreement between the approximation and the solutions are excellent across the full range of contact angles, being always within 0.1% for a 2.5× objective and within 1% for a 10× objective. Note that d^l passes zero at $\theta \approx 60°$ (i.e. the light source is focused onto the substrate surface), meaning caution must be taken of multiple solutions of $\theta(d^l, D)$.

It is possible to perform a similar analysis for the refractive mode, modelling the droplet as a thick refractive lens. This analysis is presented in the Supporting Information. However, as can be seen in Figure 4, agreement with numerical predictions is poor except for the case of extremely low-NA objectives. Therefore, we recommend use of a numerical technique to calculate contact angles above 10° in the refractive mode.

2.3 Numerical solution

Code to verify a possible solution for the values (D, d^l, θ) for a given NA and z_0 in the reflective mode may use the following logic, assuming axial symmetry to reduce the problem to two dimensions:

1. calculate the intercept of the droplet interface and a line of angle φ_c which intercepts the focal plane at $r = \frac{1}{2}d^l$;
2. calculate the surface angle α at this point;
3. estimate the incoming angle of light φ_i required to satisfy the reflection condition;
4. compare this to the expected φ_i calculated from z_o.

A solution may be found for a given (D, d^l) by trying a range of θ between $0°$ and $90°$ and iteratively homing in on the range containing the solution, if one (or more) exist. A similar approach works for the refractive mode, except now the logic runs:

1. calculate the intercept of the droplet interface and a line of angle $-\varphi_c$ intercepting the focal plane at $r = \frac{1}{2}d^r$;
2. calculate the surface angle α at this point;
3. estimate the angle of light β required to satisfy the refraction condition;
4. find the intercept of the mirror image of the droplet interface in the focal plane and a line of angle β passing through the first intercept point;
5. calculate the surface angle α at this new point;
6. estimate the incoming angle of light φ_i required to satisfy the refraction condition;
7. compare this to the expected φ_i calculated from z_o.

Results are shown in Figure 4 for water drops in air under three different objectives.

3 Experimental procedure

The technique may be used to measure the contact angle of any droplet provided it meets three criteria. Firstly, the droplet must be small enough that gravitational influence on its profile may be neglected, and it may be assumed with reasonable accuracy to form a spherical cap. Typically, this is true for droplets below about 4 mm diameter, as discussed later. Secondly, the substrate must be sufficiently uniform for the contact line to be approximately circular. Finally, the contact angle must be well below $60°$. It may be seen from Figure 4 that in the reflective mode d^l passes zero close to $60°$, and in the refractive mode d^r also passes a minimum at a similar angle. Thus every value of d^l, D has two possible solutions for θ: one above $60°$ and one below. This could lead to ambiguity in estimating θ for angles too close to $60°$. It is assumed that far from this angle there is little scope for ambiguity: whilst it can be imagined that there might be confusion whether a droplet has a contact angle (for example) either $55°$ or $66°$, for angles below $30°$ the

6

other solution would have $\theta > 90°$, a possibility which could be easily ruled out by (for example) looking from the side with the naked eye.

Illumination must be in reflected rather than transmitted mode, and the optical aperture must be set to a very small opening otherwise the boundary between the light and dark regions will appear highly diffuse. A suitable objective lens needs to be chosen to match both the size of the droplet and the contact angle to be measured. Low-magnification objectives tend to have small NA and may measure very small contact angles and view large-diameter droplets. High-magnification objectives tend to have larger NA and can make more precise measurements of larger contact angles for smaller droplets. The best objective to use for any particular drop is typically the highest-NA objective which can measure the required angle and also can fit the droplet within its field of view.

It is therefore useful to estimate the minimum contact angle $\theta_{\min}$ an objective can measure. This can be found from its NA using the thin film approximation, which becomes quite accurate as the droplet thickness approaches zero near the contact line. From Equation 5, given that $d^l = D$ and approximating $z_o \approx \infty$:

$$\theta^l_{\min} \approx \frac{NA}{2n_m} \tag{17}$$

and for the refractive mode, making an equivalent step from Equation 8:

$$\theta^r_{\min} \approx \left(\frac{n}{n_m} - 1\right)^{-1} \frac{NA}{2n_m}. \tag{18}$$

It is important that the focal plane is coincident with the substrate surface. This is easily achieved by focusing on the contact line at the edge of the droplet. The droplet may then be photographed and the values D, d^l and/or d^r measured from the image.

3.1 Estimation of optical parameters

Where great precision is not required, z_o may be assumed to equal infinity and NA is stated on most microscope objectives. Finite z_o is a significant correction only when measuring very low angles with low-NA objectives, and through testing a selection of different objectives we have found the stated NA to be consistently accurate to within 2.5%. However in order to decrease the potential for error, it is usually desirable to measure these parameters.

We have devised a simple technique for measuring NA: if a light source is shone through the camera port of a microscope, it will project a well-defined cone of light through the objective lens, of half-angle φ_c, relating to NA through Equation 1. If a prism or mirror is placed on the stage to project this horizontally onto a vertical screen then φ_c may be measured by measuring the diameter of the bright region on the screen, with the screen at two distances from the microscope of known separation.

Measurement of z_o may be performed by focusing the microscope on an opaque substrate with two closely spaced pinholes. A screen (or CCD sensor) placed a known distance below the pinholes will be illuminated by two bright spots; the separation of the centres of these spots will be slightly larger than that of the two pinholes. By measuring the separation between the pinholes and that between the bright spots on the screen, z_o may be estimated through simple geometry.

4 Experimental validation

Experiments were performed on a Zeiss Axio Scope.A1, fitted with 2.5×, 5× and 10× "Epiplan" objectives as detailed in Table 1. To test the generality of the technique beyond this specific instrument, some measurements have also been taken using a Vickers Instruments M17 fitted with a 2.5× objective.

Freshly cleaved Muscovite mica was used as a test substrate because of its flatness and chemical uniformity[19], making it simple to produce large, perfectly round drops without need of elaborate cleaning procedures. Mica is a transparent substrate, and a thin sheet of it (below 50 µm) was cleaved and placed onto a glass slide with a layer of hexadecane between the two. The hexadecane pulled the mica flat against the glass and reduced the reflection that would have been the consequence of a mica-air-glass transition. As the thickness of the mica substrate is very small, it is expected that the presence of a mica-hexadecane-glass interface will not significantly affect the refracted mode measurements. The back surface of the glass slide is painted in black enamel to prevent reflection. Droplets are applied to the mica surface using a pipettor.

As seen in Figure 1, the boundary of the bright circles is not completely sharp, and therefore there is an uncertainty in d^l and d^r, which is typically the largest single source of experimental uncertainty. Error bars in this and subsequent experiments are calculated by measuring both a largest and a smallest feasible value for d from a single image, and calculating θ for both; the mean θ is taken with an uncertainty spanning 68% of the range between the two extremes. This is combined in quadrature with a 1.5% error representing uncertainty in measurement of NA. Errors in refractive index (refractive mode only), from imperfect focus or from deviation from a perfect spherical profile are not included in error bars, as they are difficult to quantify and expected to be smaller than other sources of error.

To compare the two modes and different objectives, a drop of triethylene glycol was used as a test liquid. Triethylene glycol has a negligible vapour pressure, producing a droplet of static volume and contact angle. As it is hygroscopic, a dish of the liquid was left for two weeks in a laminar flow cabinet to equilibrate with atmospheric moisture. A small correction to the refractive index was than made based on an ambient humidity measurement, Raoult's law, and literature data on water-triethylene-glycol-mixture refractive index[20].

Images were taken of a droplet using alternating objectives, with each image providing a measurement of both the reflective and the refractive mode. θ was calculated using the numerical method, as was the case for all experimental tests. Figure 5 shows the results. It can be seen that the reflective and refractive modes are consistent with one another, and that the size of the error for each is comparable. There is also consistency between the three different objectives, but there is a lower experimental error for the higher-magnification, higher-NA objectives.

In order to test how the technique operates over a range of different contact angles, it was desirable to use a liquid with a contact angle which would vary over time. For this purpose, hexadecane droplets were studied. Hexadecane spreads slowly if applied to mica, so that a droplet has an increasing D and decreasing θ. As it should not appreciably evaporate over this time period, its volume should remain constant. This is shown in Figure 6a. The black points show measurement of the decreasing contact angle, and the green points are the corresponding droplet volumes calculated from measured D and θ, assuming a spherical cap profile. If the contant angle measurements are accurate then the volume should be invariant with time. This is approximately true, but there is a decrease in calculated volume with time just on the upper limit of that consistent with expected experimental error. It is not clear whether this is due to a small error in contact angle measurement or whether there is some slight evaporation over time.

Figure 6a shows another feature of the technique: for any given objective, the uncertainty decreases as the measured contact angle decreases. For these data there appears to be an approximately constant relative error on θ of about 3.5%.

Two attempts are made to compare contact angles measured using our technique to those found using an established technique. One, using the sessile drop technique, was made with triethylene glycol on mica and is shown in Figure 5, being in good agreement with the our technique. The other is shown in Figure 6b. Again using a spreading drop of hexadecane, the reflected mode is compared to the contact angle calculated from the spacing of interference fringes near the contact line in reflected 532 nm light. Images are taken using alternating objectives: a low-magnification lens to observe the whole drop and a high-magnification lens to observe interference fringes. Agreement between the two techniques is very good over the limited range of angles for which both techniques may be used.

It is often important to distinguish between advancing and receding contact angles. This is not always possible using our technique, but can be achieved in system-specific circumstances. A droplet pipetted onto a surface may be supposed to spread until it reaches the advancing contact angle and then stop; thus the triethylene glycol contact angles measured in Figure 5 are presumed to be advancing angles. In contrast, an evaporating droplet may be supposed to first spread to its advancing contact angle, and then reduce its volume within a fixed diameter until the receding angle is reached. An example of this is shown in Figure 7 for water evaporating on mica which has been soaked in water for one hour and then dried. Although the droplet spreading occurred

too quickly to catch, a period of evaporation at fixed diameter can be seen followed by a period of receding. The receding contact angle is the angle at which the diameter first starts to recede.

5 Discussion

The technique outlined in the previous sections is flexible; it may for example be used with substrates having either a reflective, transparent or diffusive surface. For a reflective surface (e.g. polished silicon) both modes may be used, but it is possible that the strong reflection from the liquid-substrate interface may make the reflective mode difficult to observe (Figure 8a). For a transparent surface (e.g. glass, mica) either mode may be used, but for the refractive mode care must be taken to avoid back-reflection from the reverse face of the substrate, for example by painting the reverse face black. For a diffusive surface only the reflected mode may be used as there can be no clean reflection from the liquid-substrate interface (Figure 8b). Note that the reflective mode, unlike the refractive mode, requires no knowledge of the liquid's refractive index. The reflective mode may also be the only suitable mode if the liquid and substrate have a similar refractive index (allowing little or no reflection at their interface) or if the liquid is not transparent (e.g. mercury).

Droplets must be small enough that their profile is spherical to a good approximation. The criteria for this is that the hydrostatic pressure difference between the top and bottom of the droplet should be much less than the Laplace pressure difference across the interface, i.e.:

$$hg\rho \ll \frac{2\gamma}{R} \tag{19}$$

where g is acceleration due to gravity, ρ the liquid density and γ the surface tension. Using Equations 10 and 11 and the paraxial approximation, it may be shown that for small angles, Equation 19 is approximately equivalent to

$$D \ll 4\sqrt{\frac{\gamma}{g\rho}} \tag{20}$$

In the case of water droplets, this means $D \ll 11$ mm. We therefore suggest $D \approx 4$ mm as an approximate upper limit for the size of droplets.

The technique has advantages and disadvantages over existing methods, depending on the system and on the circumstances of measurement. First, we will consider the predominant sessile drop technique. In its simplest incarnation, this involves placing a drop onto a substrate and photographing it from the side, measuring the contact angle directly using a protractor[21]. More commonly, some manner of curve fitting is used to calculate the contact angle from the drop profile, possibly using mathematical techniques to account for gravitational deformation where great precision is required[22-23]. The sessile drop technique has two key advantages over our technique: it can measure arbitrarily high contact angles, and it can distinguish advancing and

receding angles by injecting or withdrawing liquid into the drop. However, due to the camera typically being placed slightly above horizontal for practical reasons, the sessile drop technique can becoming increasingly inaccurate for contact angles below about 20°[10, 23], and our technique is therefore likely to greatly exceed its precision at small angles. In addition the sessile drop technique cannot be used when an experimental cell blocks the view from the side, or when the droplet is immersed in another liquid.

While other optical lensing techniques (as discussed in the introduction) may provide a higher level of precision than our microscopical technique, they require a specialised setup and may not be appropriate in applications where dynamic imaging of the droplet is required during a time-dependent process, or several small droplets are to be observed simultaneously. Another optical technique is to infer the contact angle from thin-film interference at the very edge of the drop[24-26]. The simplest version of this technique is to observe interference fringes under a microscope, as was used previously in Section 4. This is extremely accurate and has the advantage that there is no minimum observable contact angle. However it suffers from being only applicable for extremely low contact angles (anything above 5–7° for typical n is difficult, in our experience), and for all except the very lowest angles fringes are only observable by focusing on the very edge of a drop using a high-powered objective. Thus our technique is preferable if whole-drop observation is required. Another microscopical technique was put forward by Fischer and Ovryn which used a similar analysis to our own to model light refractively lensing through a drop, but required a scanning confocal interference microscope to measure phase shifts[27].

Another set of measurement techniques involves the use of surface tension effects to measure contact angle. This includes the Wilhelmy technique in which a substrate is drawn into and out of the liquid[28-29], and a technique which measures the shape of a capillary bridge between two surfaces[30]. Such techniques are typically not useful for dynamic measurements, or for localised measurements, and require knowledge of the surface tension and density.

There is an even simpler way to estimate a droplet's contact angle from a top-down view than the one described here: calculation from a known volume and diameter[31-34]. This has the advantage of working over a wide range of contact angles and even above $\theta = 90°$, as well as not requiring knowledge of the objective lens' optical parameters, however it has one obvious downside: it requires precise knowledge of the droplet's volume. Dispensing droplets on the microlitre scale with small uncertainty in volume is a difficult technical challenge. The technique also lacks potential to study evaporating droplets whose volume changes with time, or droplets applied through condensation or through a spray whose volume is not even approximately known.

6 Conclusion

We have outlined a procedure for a method of contact angle measurement using only an optical microscope, and requiring no knowledge of a droplet's volume, density or surface tension (or even, in the reflective mode, its refractive index). A theoretical model has been developed, and

shown to be consistent with experimental tests. The technique is recommended for the range 2–30°, but this is not a firm limit: angles below 2° may be measured with the use of an unusually low-*NA* objective, and measurement of angles above 30° is possible, but is associated with increasingly large uncertainty such that other techniques are likely to be preferable. There is also an increasing problem of potential ambiguity arising from multiple solutions for θ as θ approaches 60°.

The technique should be useful as a surface characterisation technique for small angles where the sessile drop technique is imprecise. Numerous scientifically and technologically important classes of materials exhibit low water contact angles, including metals, glasses and clay minerals. Measurement of low contact angles is a useful tool to indirectly study the imperfections of a surface or to test its cleanliness, as the contact angle on a hydrophilic surface is often very sensitive to small amounts of contamination or minor chemical modification[35-37]; this sensitivity can also make it a useful tool for measuring surface energies [8-9]. The technique is highly versatile, allowing measurement of liquid-liquid-solid contact angles and able to track changes in contact angle with time. As it is naturally coupled with microscopic observation, it naturally lends itself to experiments where dynamic observation of processes within droplets is required, such as the freezing of supercooled droplet arrays[38-39] or precipitation from evaporating drops[40-41].

Acknowledgements

Table 1. Stated (NA_s) and measured (NA_m) values of NA, and also measured z_0 for objectives used in experiments.

Objective	Serial number	NA_s	NA_m	z_0 (mm)
Zeiss 2.5×	422320-9900	0.06	0.0585	190
Zeiss 5×	422030-9902	0.13	0.131	340
Zeiss 10×	422040-9902	0.25	0.255	67
Vickers 2.5×	V579	0.08	0.0805	129
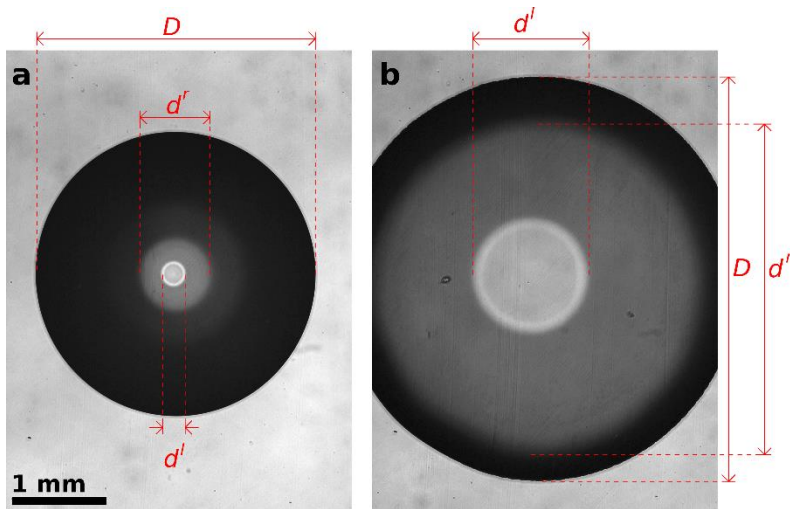
Figure 1. Two photographs of a 0.75 µL drop of hexadecane spreading on Muscovite mica under a 2.5× Zeiss objective. The inner bright circle (diameter d^l) corresponds to the reflected mode; the outer (diameter d^r) to the refractive mode. From these and the contact diameter (D), the contact angles are estimated to be (a) 17.5° and (b) 5.6°.
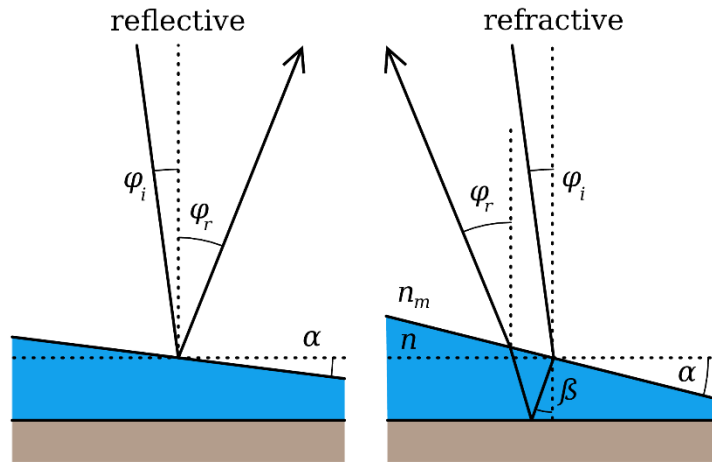
Figure 2. Illustration of reflection and refraction of light from a thin angled film. If the surface angle α is above a certain threshold, then the reflected angle φ_r will exceed the critical angle φ_c for the objective lens and the film will appear dark.
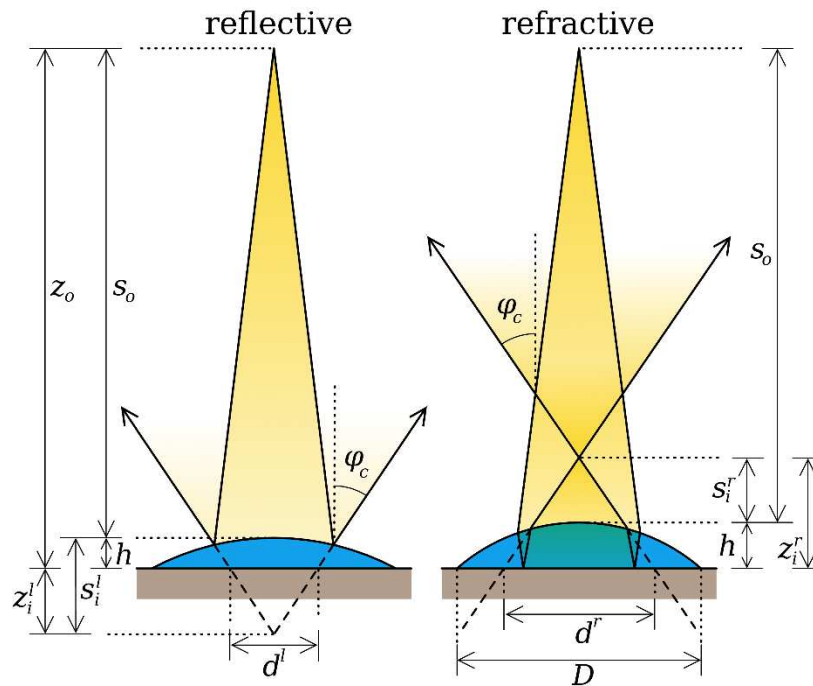

Figure 3. Illustration of droplets acting as lenses to focus incoming light. In the reflective mode, the droplet surface creates a virtual image of the light source a distance s_i^l below the liquid surface. In the refractive mode, the droplet effectively acts as double-convex lens to create a real image a distance s_i^r above the surface.
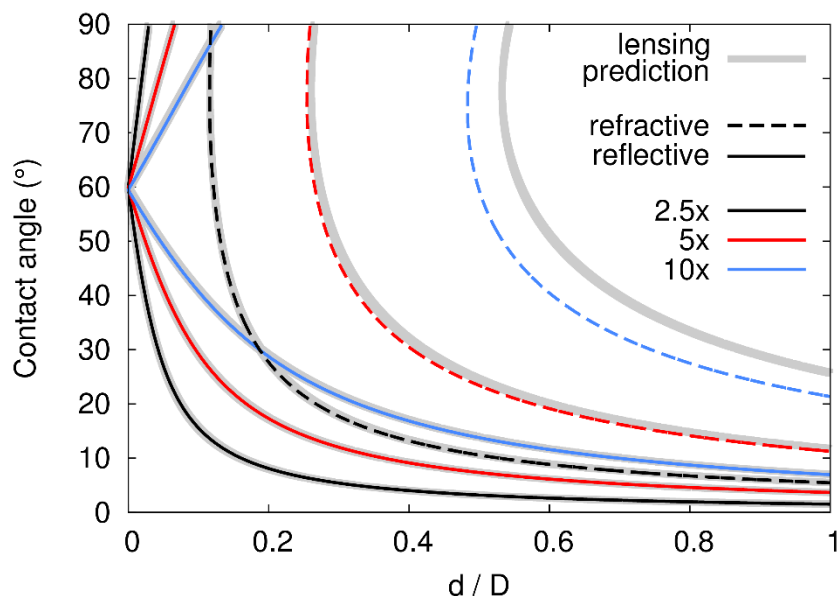
Figure 4. Graph showing predicted contact angle as a function of d/D for $D = 2$ mm droplets of water ($n = 1.333$) in air under 2.5×, 5× and 10× Zeiss objectives in both reflective and refractive modes. Black, red and blue lines are calculated using a numerical approach. The thick grey lines show the predictions of the lensing approximation for comparison.
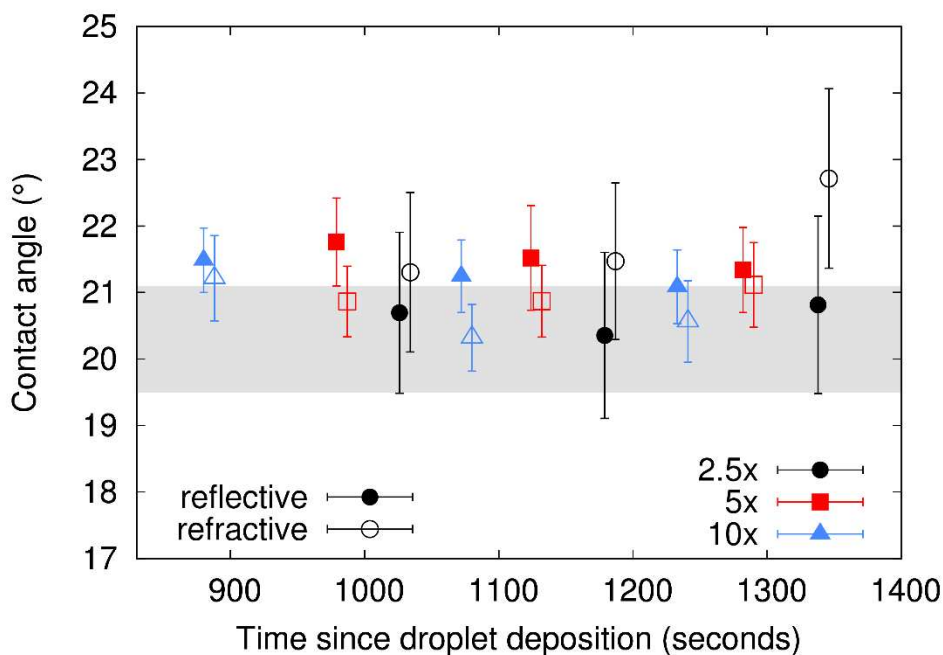

Figure 5. Comparison between 2.5×, 5× and 10× Zeiss objectives and between the reflective and refractive modes for estimating the contact angle of a static 0.1 µL drop of triethylene glycol on mica. Each pair of reflective/refractive mode measurements is taken from a single image; the small time offset between them is only for visual clarity. Error bars on refractive mode points do

not include any uncertainty in refractive index. The grey region represents the uncertainty range on a measurement using the sessile drop technique on a similar substrate ($20.3 \pm 0.8°$).
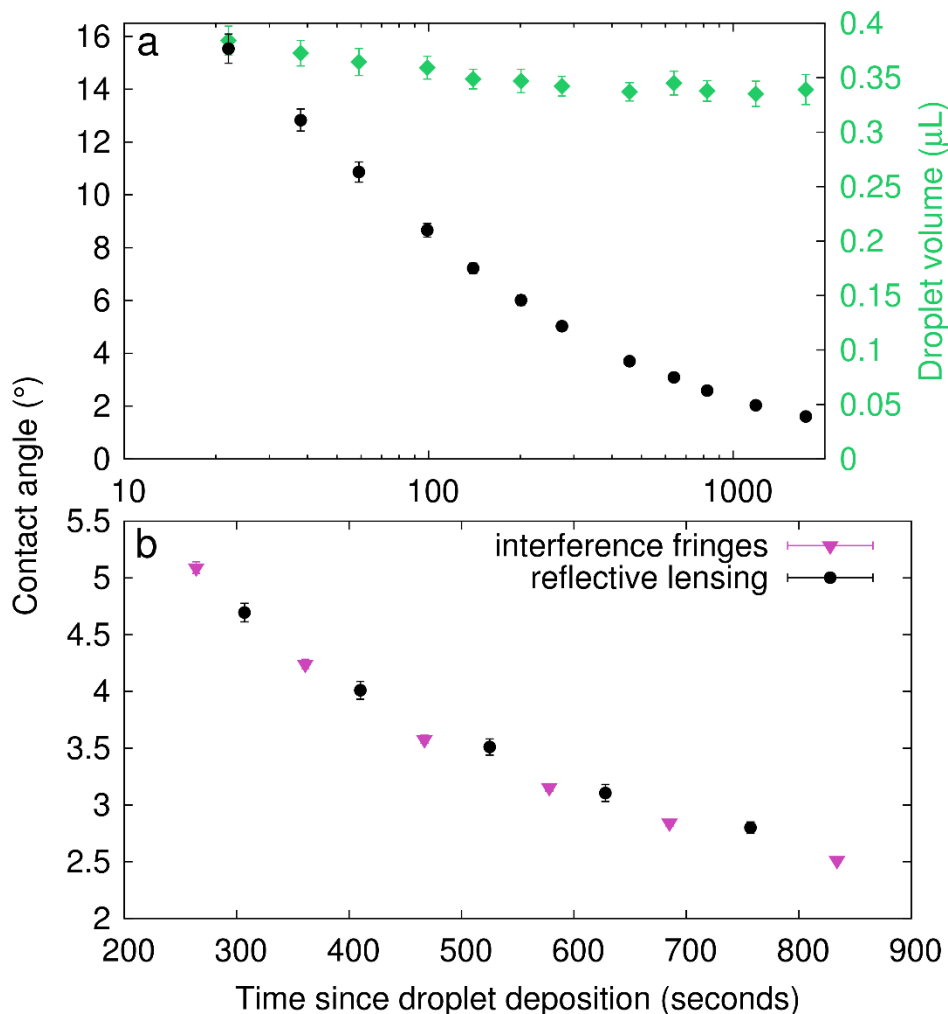

Figure 6. Contact angle measurements (reflective mode, 2.5× Zeiss objective) for two droplets of hexadecane ($n = 1.434$) spreading on mica. (a) also shows the droplet volume (green diamonds), estimated from the measured contact angle and diameter, remaining approximately constant as the droplet spreads. (b) also shows the contact angle (purple triangles) measured from interference fringes at the droplet's edge for comparison; error bars on these points do not include any uncertainty in refractive index.
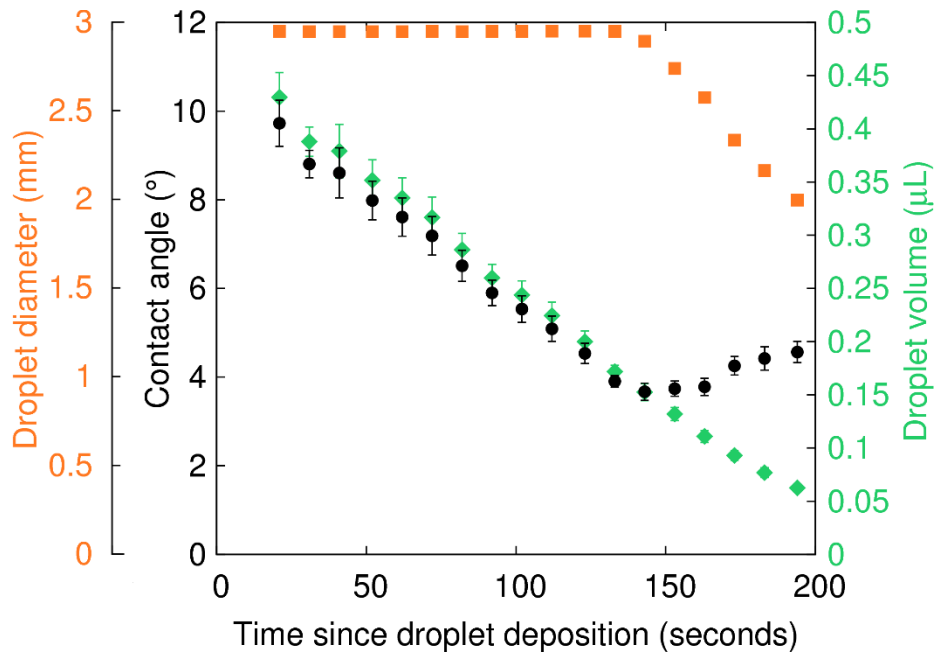
Figure 7. Diameter (orange squares), contact angle (black circles) and volume (green diamonds) of an evaporating water droplet on mica. The droplet diameter begins to reduce when the receding contact angle is reached. Contact angles are measured using a 2.5× Vickers objective in reflective mode.
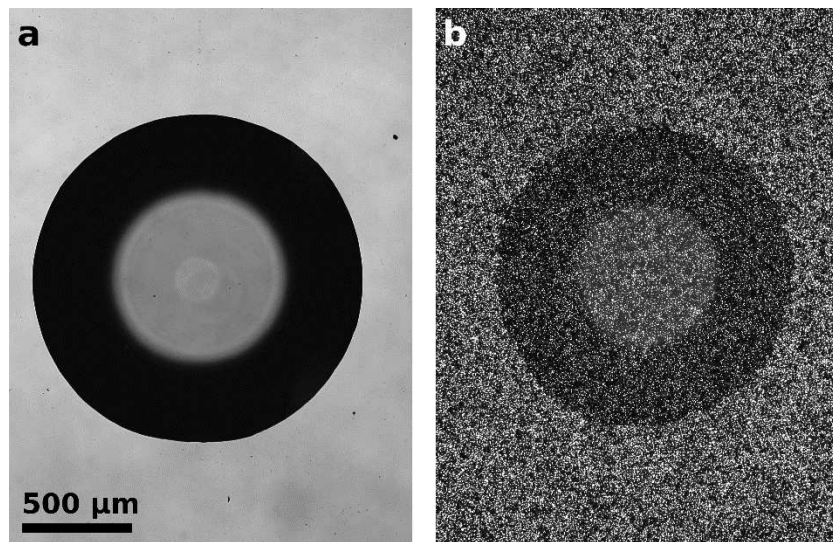

Figure 8. Water droplets on (a) polished silicon and (b) rough silicon, imaged using a 5× Zeiss objective. The reflective polished silicon has a clear refractive mode circle, and a fainter reflective mode circle visible within, predicting $\theta = 23.1 \pm 0.8°$ and $23.6 \pm 0.9°$ respectively. The diffusive surface of the rough silicon does not produce a refractive mode circle, but the reflective mode predicts $\theta = 8.2 \pm 0.7°$.

17

(1) Herminghaus, S. Dynamics of wet granular matter. *Adv. Phys.* **2005,** *54* (3), 221-261.

(2) Culligan, E. M.; Christenson, H. K. Cohesion of granular matter in subzero humidity. *J. Phys. Chem. C* **2014,** *118* (29), 15929-15933.

(3) Dullien, F. A. L. *Porous media: fluid transport and pore structure*, Academic press: 2012.

(4) Hillel, D. *Fundamentals of soil physics*, Academic press: 2013.

(5) Campbell, J. M.; Ozturk, D.; Sandnes, B. Gas-Driven Fracturing of Saturated Granular Media. *Phys. Rev. Appl.* **2017,** *8* (6), 064029.

(6) Rioboo, R.; Tropea, C.; Marengo, M. Outcomes from a drop impact on solid surfaces. *Atomization Spray* **2001,** *11* (2), 155-165.

(7) Redon, C.; Brochard-Wyart, F.; Rondelez, F. Dynamics of dewetting. *Phys. Rev. Lett.* **1991,** *66* (6), 715.

(8) Good, R. J.; Girifalco, L. A. A theory for estimation of surface and interfacial energies. III. Estimation of surface energies of solids from contact angle data. *J. Phys. Chem.* **1960,** *64* (5), 561-565.

(9) Israelachvili, J. N. *Intermolecular and Surface Forces*, Academic Press: 1992.

(10) Chau, T. T. A review of techniques for measurement of contact angles and their applicability on mineral surfaces. *Miner. Eng.* **2009,** *22* (3), 213-219.

(11) Yuan, Y.; Lee, T. R. Contact angle and wetting properties. In *Surface science techniques*; Springer: 2013; pp 3-34.

(12) Allain, C.; Ausserre, D.; Rondelez, F. A new method for contact-angle measurements of sessile drops. *J. Colloid Interf. Sci.* **1985,** *107* (1), 5-13.

(13) Zhang, N.; Chao, D. F. A new laser shadowgraphy method for measurements of dynamic contact angle and simultaneous flow visualization in a sessile drop. *Opt. Laser Technol.* **2002,** *34* (3), 243-248.

(14) Zhang, N.; Chao, D. F. Caustics and caustic-diffraction in laser shadowgraphy of a sessile drop and identification of profile near contact line. *Opt. Laser Technol.* **2003,** *35* (3), 155-161.

(15) Thomas, L. P.; Gratton, R.; Marino, B. M.; Diez, J. A. Droplet profiles obtained from the intensity distribution of refraction patterns. *Appl. Optics* **1995,** *34* (25), 5840-5848.

(16) Israel, S. C.; Yang, W. C.; Chae, C. H.; Wong, C. Characterization of polymer surfaces by laser contact-angle goniometry. *ACS Polym. Prep.* **1989,** *30*, 328.

(17) Awasthi, A.; Bhatt, Y. J.; Garg, S. P. Measurement of contact angle in systems involving liquid metals. *Meas. Sci. Technol.* **1996,** *7* (5), 753.

(18) Tachon, L.; Guignard, S. An accurate optical method for the measurement of contact angle and interface shape of evaporative thin liquids films. *Exp. Therm. Fluid Sci.* **2018,** *90*, 66-75.

(19) Christenson, H. K.; Thomson, N. H. The nature of the air-cleaved mica surface. *Surf. Sci. Rep.* **2016,** *71* (2), 367-390.

(20) Chiao, T.-T.; Thompson, A. R. Densities and Refractive Indices for Glycol-Water Solutions... Triethylene Glycol, Dipropylene Glycol, and Hexylene Glycol. *Anal. Chem.* **1957,** *29* (11), 1678-1681.

(21) Bigelow, W. C.; Pickett, D. L.; Zisman, W. A. Oleophobic monolayers: I. Films adsorbed from solution in non-polar liquids. *J. Colloid Sci.* **1946,** *1* (6), 513-538.

(22) Huh, C.; Reed, R. L. A method for estimating interfacial tensions and contact angles from sessile and pendant drop shapes. *J. Colloid Interf. Sci.* **1983,** *91* (2), 472-484.

(23) Li, D.; Cheng, P.; Neumann, A. W. Contact angle measurement by axisymmetric drop shape analysis (ADSA). *Adv. Colloid Interfac.* **1992,** *39*, 347-382.

(24) Longman, G. W.; Palmer, R. P. Two microscopical methods of determining the contact angles of small drops. *J. Colloid Interf. Sci.* **1967,** *24* (2), 185-188.

(25) Scheid, B.; Kabov, O.; Minetti, C.; Colinet, P.; Legros, J. C. In *Measurement of free surface deformation by reflectance-Schlieren method*, Proc. 3rd Eur. Conf. Heat Mass Transfer, Heidelberg, 2000.

(26) Sundberg, M.; Månsson, A.; Tågerud, S. Contact angle measurements by confocal microscopy for non-destructive microscale surface characterization. *J. Colloid Interf. Sci.* **2007,** *313* (2), 454-460.

(27) Fischer, D. G.; Ovryn, B. Interfacial shape and contact-angle measurement of transparent samples with confocal interference microscopy. *Opt. Lett.* **2000,** *25* (7), 478-480.

(28) Wilhelmy, L. Ueber die Abhängigkeit der Capillaritäts-Constanten des Alkohols von Substanz und Gestalt des benetzten festen Körpers. *Ann. Phys.* **1863,** *195* (6), 177-217.

(29) Tretinnikov, O. N.; Ikada, Y. Dynamic wetting and contact angle hysteresis of polymer surfaces studied with the modified Wilhelmy balance method. *Langmuir* **1994,** *10* (5), 1606-1614.

(30) Restagno, F.; Poulard, C.; Cohen, C.; Vagharchakian, L.; Léger, L. Contact angle and contact angle hysteresis measurements using the capillary bridge technique. *Langmuir* **2009,** *25* (18), 11188-11196.

(31) Ryley, D. J.; Khoshaim, B. H. A new method of determining the contact angle made by a sessile drop upon a horizontal surface (sessile drop contact angle). *J. Colloid Interf. Sci.* **1977,** *59* (2), 243-251.

(32) Fisher, L. R. Measurement of small contact angles for sessile drops. *J. Colloid Interf. Sci.* **1979,** *72* (2), 200-205.

(33) Skinner, F. K.; Rotenberg, Y.; Neumann, A. W. Contact angle measurements from the contact diameter of sessile drops by means of a modified axisymmetric drop shape analysis. *J. Colloid Interf. Sci.* **1989,** *130* (1), 25-34.

(34) Dutra, G.; Canning, J.; Padden, W.; Martelli, C.; Dligatch, S. Large area optical mapping of surface contact angle. *Opt. Express* **2017,** *25* (18), 21127-21144.

(35) Schrader, M. E. Wettability of clean metal surfaces. *J. Colloid Interf. Sci.* **1984,** *100* (2), 372-380.

(36) Engländer, T.; Wiegel, D.; Naji, L.; Arnold, K. Dehydration of glass surfaces studied by contact angle measurements. *J. Colloid Interf. Sci.* **1996,** *179* (2), 635-636.

(37) Zhang, D.; Wang, Y.; Gan, Y. Characterization of critically cleaned sapphire single-crystal substrates by atomic force microscopy, XPS and contact angle measurements. *Appl. Surf. Sci.* **2013,** *274*, 405-417.

(38) Murray, B. J.; Broadley, S. L.; Wilson, T. W.; Bull, S. J.; Wills, R. H.; Christenson, H. K.; Murray, E. J. Kinetics of the homogeneous freezing of water. *Phys. Chem. Chem. Phys.* **2010,** *12* (35), 10380-10387.

(39) Campbell, J. M.; Meldrum, F. C.; Christenson, H. K. Is ice nucleation from supercooled water insensitive to surface roughness? *J. Phys. Chem. C* **2015,** *119* (2), 1164-1169.

(40) Hu, H.; Larson, R. G. Evaporation of a sessile droplet on a substrate. *J. Phys. Chem. B* **2002,** *106* (6), 1334-1344.

(41) Harrington, G. F.; Campbell, J. M.; Christenson, H. K. Crystal patterns created by rupture of a thin film. *Cryst. Growth Des.* **2013,** *13* (11), 5062-5067.